Chapter: 1

Introduction and Literature Review

1.1 Introduction

The perovskite oxides are the important class of materials which offer interesting physical phenomena and piezoelectric response for many technological applications due to their important electrical and magnetic properties. The structure of naturally obtained mineral $CaTiO_3$ is a kind of general formula ABO_3 type, called perovskite oxide [Perovski (1839)]. The well-known $BaTiO_3$ [BT], $PbTiO_3$ [PT], and $PbZrO_3$ [PZ] are the simple examples of other perovskite oxide. Perovskite solid solutions $Pb(Zr_xTi_{1-x})O_3$ [PZT], $(1-x)Pb(Mg_{1/3}Nb_{2/3})O_3-xPbTiO_3$ [PMN-PT] and $(1-x)Pb(Zn_{1/3}Nb_{2/3})O_3-xPbTiO_3$ [PZN-PT] etc. have attracted a lot of attention due to their high piezoelectric responses around the morphotropic phase boundary (MPB), and are widely used for transducers and actuators applications [Jaffe et al. (1971)]. In ferroelectric perovskites, the morphotropic phase boundary (MPB) is nearly vertical phase boundary in the temperature composition phase diagram, where the ferroelectric and piezoelectric properties are drastically enhanced due to phase coexistence and structural instability [Jaffe et al. (1971); Goldschmidt (1929)]. The structure changes abruptly and usually a crystallographic phase transition is observed around the MPB [Jaffe et al. (1971); Goldschmidt (1929)]. Amongst several ferroelectric solid solutions PZT has high Curie temperature ($T_C{\sim}380^oC$) for the MPB compositions, which is most suitable for the high temperature piezoelectric applications such as automotive industries and aerospace [Heywang et al. (2008)]. The MPB for PZT is observed at x=0.52 in

the temperature composition phase diagram. However, lead is released into environment during calcination, sintering and disposal processes of Pb-based perovskite oxide, which is highly toxic and leads to cancer and other health issues [Rödel et al. (2009)]. This has compelled the researchers to develop alternative MPB materials for piezoelectric applications with lead free or reduced lead concentration. Publications on lead-free piezoceramics in refereed journals for the time span from 1950 to November 2008 is shown in Fig. 1.1. As can be seen from Fig. 1.1, the number of publication on lead free piezoceramics in refereed journals shows increasing trends from 2000 onwards. From July, 2006, the European parliament has given directives to restrict the use or recycle of toxic materials in any kind of equipment to protect human, health and environment [Rödel et al. (2009)]. Therefore, there is a great demand to investigate lead free perovskite materials with high T_C and high piezoelectric response. Fig. 1.2 shows the relative cost and toxicity of the elements of the periodic table [Rödel et al. (2009)]. As can be seen from Fig. 1.2 the lead is cost effective but it is highly toxic. Therefore, in the present work we have used the bismuth, beside element of lead, which is not toxic and cost effective also.
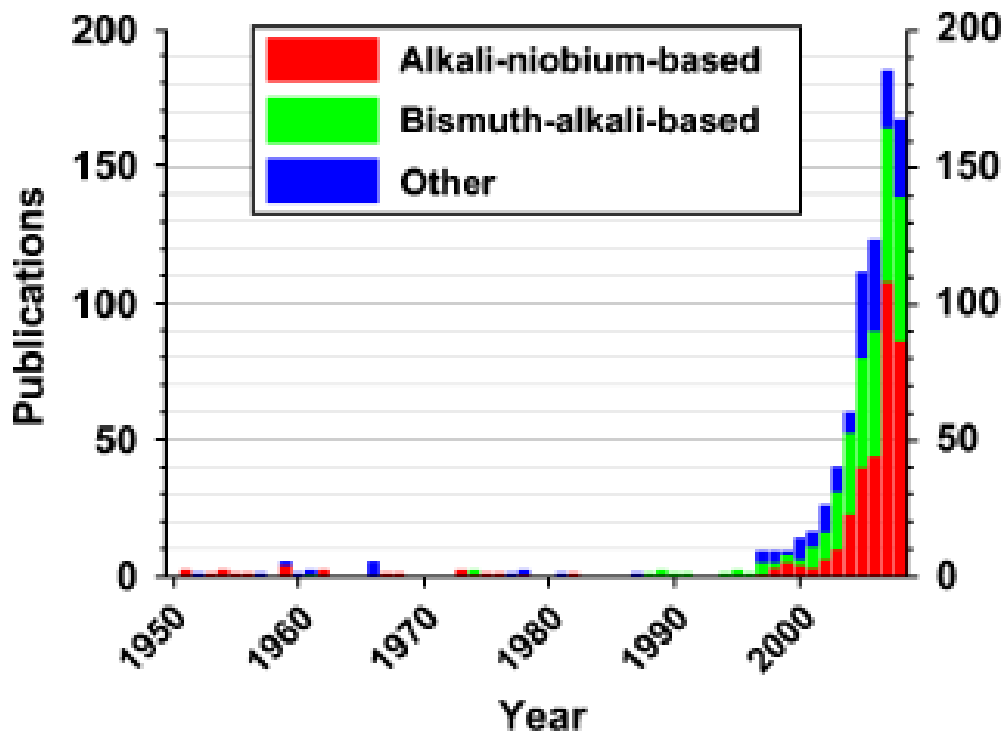
Fig.1.1 Publications on lead-free piezoceramics in refereed journals for the time spam from 1950 to November 2008 [After Rödel et al. (2009)].
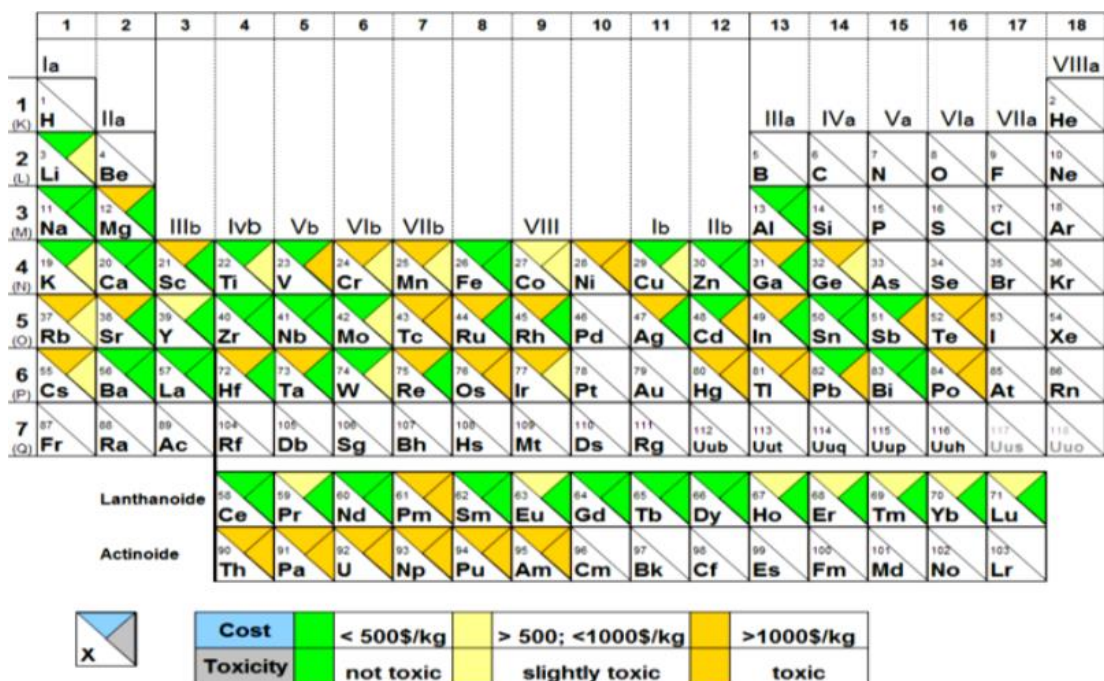

Fig.1.2 Relative cost and toxicity of the elements of the periodic Table [After Rödel et al. (2009)].

Since lead is toxic therefore, now a days the efforts are made towards the lead free or reduced lead based system with excellent ferroelectric and piezoelectric properties. In search of such materials currently extensive research are being done on bismuth based mixed perovskite solid solution with general formula $(1-x)Bi(M_1M_2)-xPbTiO_3$ where M_1 and M_2 are octahedrally coordinated transition metal cation that stoichiometrically combines to give +3 valence at B site of the perovskite structure, which shows better promises for high temperature application and good alternative of PZT. Recently several Bi-based solid solutions with reduced lead such as $(1-x)Bi(Mg_{1/2}Ti_{1/2})O_3-xPbTiO_3$ [BMT-PT], $(1-x)Bi(Mg_{3/4}W_{1/4})O_3-xPbTiO_3$ [BMW-PT], $(1-x)Bi(Mg_{1/2}Zr_{1/2})O_3-xPbTiO_3$ [BMZ-PT], $(1-x)Bi(Ni_{1/2}Ti_{1/2})O_3-xPbTiO_3$ [BNT-PT], $(1-x)Bi(Zn_{1/2}Ti_{1/2})O_3-xPbTiO3$ (BZT-PT), $Bi_{1/2}Na_{1/2}TiO_3$ and solid solutions based on them, etc. have been investigated for piezoelectric applications close to MPB. Amongst all these system BMT-PT possess high Curie temperature ($T_C \sim 430^oC$), good value of $d_{33} \sim 225pC/N$, large tetragonality (c/a=1.034) and large coercive field $E_C \sim 50kV/cm$, being more suitable for high temperature piezoelectric applications [Randall et al. (2004); Chen et al. (2009); Snel et al. (2005)].

The present thesis deals with a complete study of bismuth based mixed perovskite solid solutions $(1-x)Bi(Mg_{1/2}Ti_{1/2})O_3-xPbTiO_3$ [BMT-PT] and $(1-x)Bi(Mg_{1/2}Zr_{1/2})O_3-xPbTiO_3$ [BMZ-PT] including synthesis, crystal structures, dielectric properties, and nature of phase transitions. In this chapter, we briefly introduce the basic concepts and definitions of ferroelectrics and relevant topics. Then, we will present a brief review of literature on $(1-x)Bi(Mg_{1/2}Ti_{1/2})O_3$-

xPbTiO$_3$ [BMT-PT] and (1-x)Bi(Mg$_{1/2}$Zr$_{1/2}$)O$_3$-xPbTiO$_3$ [BMZ-PT] solid solutions.

1.2 Perovskites structure

Materials with general formula ABO$_3$ having structure similar to perovskite mineral CaTiO$_3$, where the coordination number of A-site is twelve and coordination number of B-site is six as shown in Fig. 1.3. The charge of 'A' and 'B' cations combines to give an average +6 valence in order to balance the negative charges of the 3O^{2-} to maintain the charge balance and stoichiometry of perovskite structure. The ideal perovskite structure consists of a primitive cubic unit cell, where 'A' cation occupy the cube corners, oxygen anion at each six faces and 'B' cation at the centres. Goldschmidt in 1926 proposed tolerance factor for the stability of ABO$_3$ perovskite structure [Goldschmidt (1926)]. According to Goldschmidt the ionic radii R$_A$, R$_B$ and R$_O$ of the A, B, and O ions must have to satisfy the following relationship for the stable perovskite oxide, considering cubic closed packing of ions:

$$t = \frac{(R_A + R_O)}{\sqrt{2}\ (R_B + R_O)}$$ ………………. 1.1

Where, 't' is called the tolerance factor. The perovskite structure is stable if the value of 't' lies in the range 0.80<t<1.1. The ideal cubic perovskite structure belongs to Pm3m space group symmetry, with the value of t~1. If the value of t>1 then the structure of perovskite may be tetragonal. The structure of the perovskite is expected to rhombohedral or monoclinic if the value of t<1.
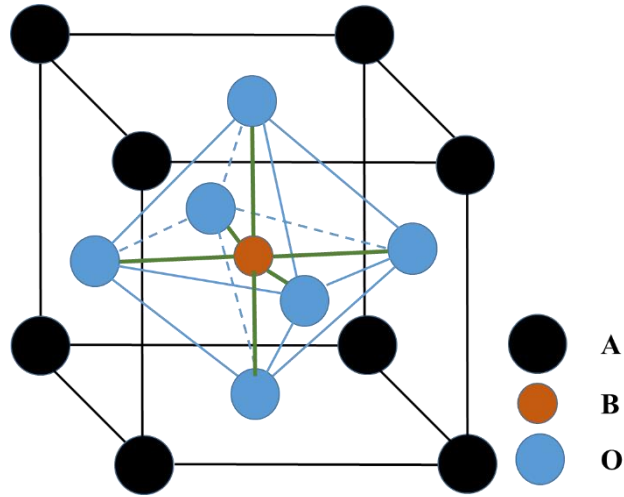
Fig.1.3 Cubic prototype perovskite oxide ABO_3 unit cell.
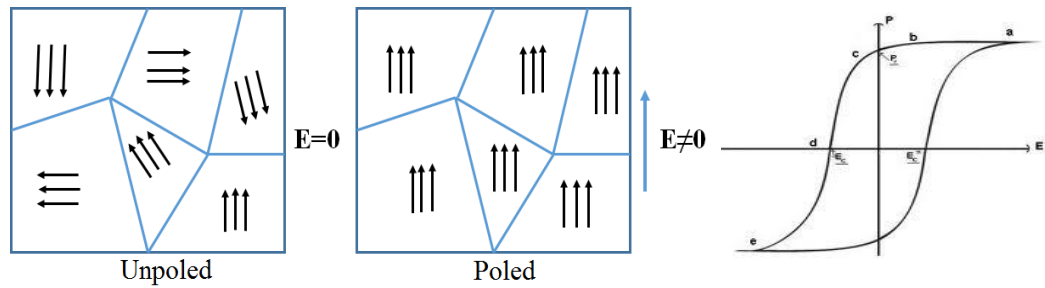
1.3 Ferroelectrics

Ferroelectric (FE) materials possess a spontaneous polarization even in the absence of an external electric fields, which is stable and can be switched hysteretically by an externally applied electric field. Most of the properties of ferroelectric materials are analogous to ferromagnetic materials such as polarization (P) corresponding to magnetization (M), electric field (E) corresponding to magnetic field (H), and electric displacement (D) corresponding to magnetic flux density (B). When external electric field is applied to a ferroelectric material, domains start to align in the direction of field hence polarization starts increasing from zero value. For sufficiently high electric fields, polarization reaches to saturation polarization (P_s) and reducing the field to zero leaves the material with remanent polarization (P_r). When the direction of field is

reversed, polarization is first reduced to zero and the field required to make remanent polarization zero is called coercive field (E_C), then higher electric field changes polarization direction as saturation polarization in the opposite direction as shown in Fig. 1.4. The FE material undergoes a phase transformation from a high temperature paraelectric phase to low temperature ferroelectric phase due to development of polar axis via a structural phase transformation [Jaffe et al. (1971)]. Above Curie point, hysteresis loop disappears. The BaTO$_3$ [BT] possess the FE ordering and the hysteresis loop at room temperature. The structure of BT is tetragonal (space group P4mm) at room temperature. Above the transition temperature (T_C) the paraelectric (cubic) phase is observed. Above T_C, The ferroelectric materials obeys the Curie-Weiss law

$$\varepsilon^{/} = C/(T\text{-}T_C) \qquad\qquad \text{.................. 1.2}$$

Where, '$\varepsilon^{/}$' is the dielectric permittivity, 'C' and 'T_C' are Curie constant and Curie temperature respectively. The temperature above which, hysteresis loop disappears is called Curie point (T_0). Structural phase transformation occurred around the Curie point. In the case of a first order ferroelectric phase transformation the Curie temperature and Curie point are not identical but the Curie temperature (T_C) is lower than Curie point (T_0), while in case of second order ferroelectric phase transformation the two temperatures are identical i.e. T_C=T_0 [Lines et al. (1977)]. Like BaTiO$_3$ [BT], PbTiO$_3$ [PT] and KNbO$_3$ [KN] also undergo ferroelectric phase transformations.

7

Fig.1.4 Diagram of polarization process of ferroelectrics and hysteresis of polarization (P) vs. electric field (E) loop.
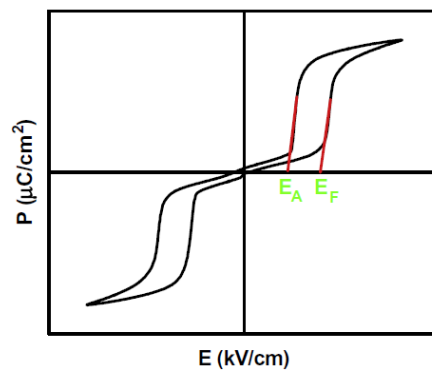
Fig.1.5 Electric-field induced polarization hysteresis loop of Anti-Ferroelectrics.

1.4 Anti-Ferroelectrics

Anti-ferroelectric (AFE) materials possess ordered dipole moments that cancel each other completely within each crystallographic unit cell. AFE materials do not have spontaneous polarization but they show sublattice polarization. The sufficiently high electric field can develop polarization in the AFE material. The AFE materials show 'twin' P-E hysteresis loops unlike ferroelectric materials as shown in Fig. 1.5. $PbZrO_3$ [Jona et al. (1957)] and $NaNbO_3$ [Cross et al. (1955)] are the example of AFE materials. In an anti-ferroelectric phase transition, the ionic displacement occurs in equal and opposite directions in pairs. Thus the unit cell of the AFE phase becomes multiple of the unit cell of the prototype paraelectric phase giving rise to the appearance of characteristic superlattice reflections in the diffraction pattern. The transition temperature is commonly known as Neel temperature (T_N) for these materials in analogy with the Neel temperature of antiferromagnetic materials.

1.5 Relaxor-Ferroelectrics

Relaxor ferroelectrics or relaxors are a class of disordered crystalline materials that have peculiar structure and properties. Relaxor ferroelectrics have a diffuse and very high value of dielectric permittivity (ε) with a significant frequency relaxation in dielectric permittivity vs temperature (T) response. Relaxor ferroelectrics solid solutions have been very much interesting over the last few decades due to their superior piezoelectric properties compared to other piezoelectric ceramics. Relaxors have slim hysteresis loop and existence of polarization above peak temperature (T_m') in the permittivity vs temperature

response. The large dielectric constants (ε), electrostrictive coefficients and electro optic constants of relaxor ferroelectrics make them ideal for super capacitors, electrostrictive actuators, biomedical transducers and optical modulators. The differences between ferroelectrics and relaxors are highlighted in table 1.1. The normal ferroelectrics possess well saturated polarization-electric field (P-E) hysteresis loop, while the relaxor ferroelectric have the slim type P-E hysteresis loop.

Table 1.1: Difference between properties of normal ferroelectrics and relaxor perovskite ferroelectrics [After Cross (1987)].

Ferroelectrics	Relaxor Ferroelectrics
Well define PE square hysteresis	Slim loop in PE hysteresis
P_R and P_S vanishes at T_C	P_R and P_S remains above T_m
Sharp phase transition	Diffused phase transition
T_C does not vary with frequency	Temp. at which the dielectric constant is maximum shifts to higher temperature with increase in frequency

A large number of relaxors ferroelectrics are Pb-based perovskite type materials which have general formula $Pb(B_1B_2)O_3$, where B_1 have lower valency cation (like Mg^{2+}, Zn^{2+}, Ni^{2+}, Fe^{3+}) and B_2 have higher valency cation (like Nb^{5+}, Ta^{5+}, W^{5+}) [Cross (1987), (1994); Smolenskii (1970)]. $Pb(Mg_{1/3}Nb_{2/3})O_3$ [PMN] [Smolenskii (1961)], $Pb(Mg_{1/3}Nb_{2/3})O_3-xPbTiO_3$ [PMN-PT] [Singh et al. (2007)],

Pb($Mg_{1/3}Ta_{2/3}$)O_3 [Bokov et al. (2006)], Pb($Sc_{1/2}Ta_{1/2}$)O_3 [Chu et al. (1993)], etc. are some examples ferroelectrics which are relaxors. In general, the normal FE show the structural phase transformation if there is any anomaly in dielectrics measurement, but in case of relaxos it is not so. The peak in real part of dielectric constant is a manifestation of the slowing down of the dipolar motion below T_m [Samara (2003)]. The peaks in the dielectric constant has been interpreted in terms of polar nano regions. Polar nano regions gives rise to diffused scattering in neutron and x-ray diffraction patterns. The temperature dependent real and imaginary part of dielectric permittivity measured at different frequencies in a crystal of the prototypical relaxor PMN is shown in Fig. 1.6. In case of PMN, the nano polar region exhibit local rhombohedral symmetry [Mathan et al. (1991)] and size distribution of these nano polar regions give rise to dielectric relaxation in frequency temperature dependence of permittivity. The polar nano regions with randomly distributed directions of dipole moment appear below Burns temperature (T_B) [Burns et al. (1983)] and the state is known as ergodic relaxor in which the polar nano regions are mobile. Above the Burns temperature the relaxors exist in non-polar paraelectric state, which is similar to paralectric state of normal ferroelectric. Around the temperatures close to T_B the polar nano regions are mobile and their behaviour is ergodic. On further cooling the dynamics of polar nano regions slows down and at the low temperature T_f , known as freezing temperature the polar nano regions freezes into nonergodic state, while the average symmetry of the materials still remains cubic [Bokov and Ye (2006)].

11

The dielectric relaxation in relaxors has been classified into two categories depending on the freezing of the polar clusters.

(i)   Vogel-Fulcher type behaviour [Vogel (1921); Fulcher (1925)]

(ii)   Arrhenius type behaviour [Bokov et al. (2006)]

The Vogel-Fulcher type and Arrhenius type behaviour are governed by equations (1.3) and (1.4), respectively.

$$\tau = \tau_o \, e^{E_a/k(T-T_{vf})} \qquad \dots\dots\dots\dots\dots \quad (1.3)$$

$$\tau = \tau_o \, e^{E_a/kT} \qquad \dots\dots\dots\dots\dots \quad (1.4)$$

In the above equation, E_a is the activation energy for thermally activated jump of polar clusters, τ is the relaxation time, k is Boltzmann constant and T_{vf} is Vogal-Fulcher freezing temperature. The relaxors like PMN [Viehland et al. (1991)] follows the Vogel-Fulcher law, while $(CoO)_{0.4}(Al_2O_3)_{0.1}(SiO_2)_{0.5}$ [Binder et al. (1986)] follows the Arrhenius law.
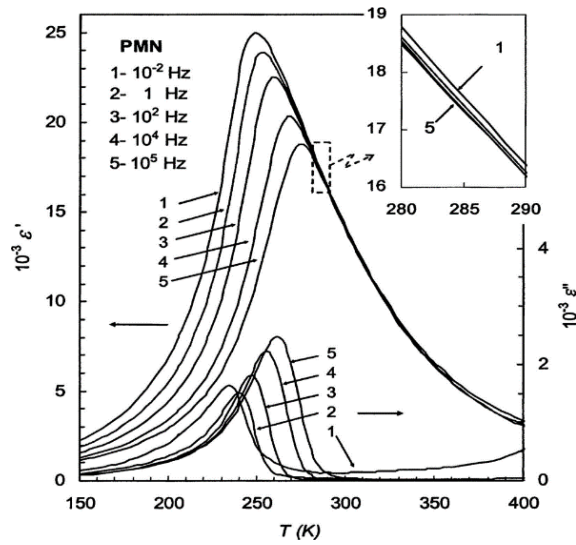
Fig.1.6 Temperature dependent real and imaginary parts of dielectric permittivity measured at different frequencies in a crystal of the prototypical relaxor $Pb(Mg_{1/3}Nb_{2/3})O_3$ [After Bokov et al. (2006)].

1.6 Piezoelectricity

Piezo originated from the Greek word piezein, which means to squeeze or press. Piezoelectricity is the ability of certain crystalline materials to develop an electric charge proportional to applied mechanical stress, discovered by Pierre Curie and Jacques Curie brother in 1880. Piezoelectric ceramics are the materials that convert electrical energy into mechanical energy and vice versa [Curie et al. (1880)]. There are two types of piezoelectric effect, direct piezoelectric effect and converse piezoelectric effect. When the change in pressure on materials detected by measuring the change in polarisation of materials, it is known as direct piezoelectric effect. Conversely, when an electronic system used to apply an electric field to physically alter the shape (strain) of materials, is known as

converse piezoelectric effect. The piezoelectric materials exhibit electromechanical coupling factor i.e. the polarization varies with an applied strain on the materials. The piezoelectric materials are very much important in the applications of sensors, actuators, transducers used in sonar and medical ultrasound, telecommunication, aerospace and automotive industries [Jaffe et al. (1971)]. The origin of the piezoelectric effect is the displacement of ionic charges within a crystal structure. When an external stress is applied, the charges are displaced and the charge distribution is no longer symmetric and a net polarization is created. The 20 crystal classes (out of 32 total) do not possess a centre of symmetry (a necessary condition for piezoelectricity to exist) i.e. non-centrosymmetric crystallographic point group shows piezoelectric effect.

1.7 Soft mode and phase transition in perovskites

Change in temperature, pressure, stress, electric field, magnetic field, composition etc. may induce the structural phase transition in perovskite type materials. The perovskite phase of $CaTiO_3$ undergoes the phase transition from orthorhombic phase to cubic phase via intermediate tetragonal phase at very high temperature ($T_C \sim 1250^oC$) [Redfern (1996)]. The perovskite phase $PbTiO_3$ also undergoes the phase transition from cubic phase to tetragonal phase on cooling below 490^oC [Shirane et al. (1970)]. In ferroelectric and anti-ferroelectric phase transitions, ions move from high symmetry site in high temperature phase to low symmetry site in low temperature phase via small displacement. Such transitions are called displacive transitions. According to Cochran (1960) and Anderson (1960), the structural phase transition can be described in terms of condensation

of soft phonon modes of the high temperature phase. The soft phonon mode is characterised by anomalous decrease in its frequency as the phase transition temperature is approached from high temperature side. Lines and Glass (1977) have given the relation for the temperature dependence of the soft phonon frequency as follow:

$$\omega^2 \propto (T\text{-}T_C) \qquad \text{……………… 1.5}$$

The structural phase transitions are classified in ferrodistortive and anti-ferrodistortive transition [Blinc et al. (1974)]. The ferrodistortive transition is the transition where the number of formula units per unit cell does not change at the transition, and the anti-ferrodistortive tansitions are the transitions where the number of formula units in the low temperature unit cell is an integral multiple of the number of formula units in the high temperature primitive cell. The ferrodistortive transitions are connected with the freezing of soft mode at the Brillouin zone centre (k=0). On the other hand the Anti-ferrodistortive transitions correspond to freezing of soft mode with a non-zero vector (k≠0) in k-space [(Lines et al. (1977); Blinc et al. (1974)]. All the structural phase transitions are associated with at least one of ten symmetry points i.e. Γ, Δ, Λ, Σ, R, T, M, S, X and Z of Brillouin zone [(Lines et al. (1977); Blinc et al. (1974)].

1.8 Morphotropic phase boundary region

Transition from one ferroelectric to other ferroelectric phase observed due to change in composition in perovskite materials can result into a morphotropic phase transition. Such transition leads a nearly vertical phase boundary in temperature-composition phase diagram known as morphotropic phase boundary

(MPB), which separates the stability region of two crystallographically different ferroelectric phases. In other words the morphotropic phase boundary in ferroelectric perovskite solid solutions is defined as a nearly vertical phase boundary in the temperature-composition phase diagram separating stability regions of two crystallographic phases. The coexistence of the neighbouring phases and maximized dielectric, piezoelectric responses are obtained for the MPB compositions. The phase coexistence region around the MPB is known as the morphotropic phase boundary region. The structure and the properties of the perovskites near the MPB is very sensitive to small changes in temperature, composition etc. The composition induced phase transition in perovskite at MPB causes the instability of the polarization state, and the polarization direction can be easily rotated by an external electric field and external stress [Fu et al. (2000); Ahart et al. (2008)] resulting giant piezoelectric responses [Bellaiche et al. (2000); Noheda et al., (2001)]. $Pb(Zr_xTi_{1-x})O_3$ [PZT] [Noheda et al. (2000)], $Pb(Mg_{1/3}Nb_{2/3})O_3$-$xPbTiO_3$ [PMN-PT] [Singh et al. (2003)], $(1-x)Bi(Mg_{1/2}Ti_{1/2})O_3$-$xPbTiO_3$ [BMT-PT] [Randall et al. (2004)], $(1-x)Bi(Ni_{1/2}Ti_{1/2})O_3$-$xPbTiO_3$ [BNT-PT] [Pandey et al. (2014)] etc. are some examples of the MPB based piezoceramics.

1.9 Recent developments in MPB based solid solutions

In PZT solid solution, it was believed that the morphotropic phase boundary separates the two crystallographic phase of rhombohedral (space group R3m) and tetragonal (space group P4mm) structure, and the coexistence of these two phases is observed around the MPB region at room temperature [Jaffe et al. (1971)]. The

phase diagram and dielectric constant and planar coupling coefficient vs. composition for the PZT piezoceramics reported by Jaffe et al. (1971) is shown in Fig. 1.7 (a) and Fig. 1.7 (b). As can be seen from Fig. 1.7 the MPB separates the rhombohedral and tetragonal ferroelectric phases and the maximization of the piezoelectric responses is found around the MPB.

(a)   **(b)**
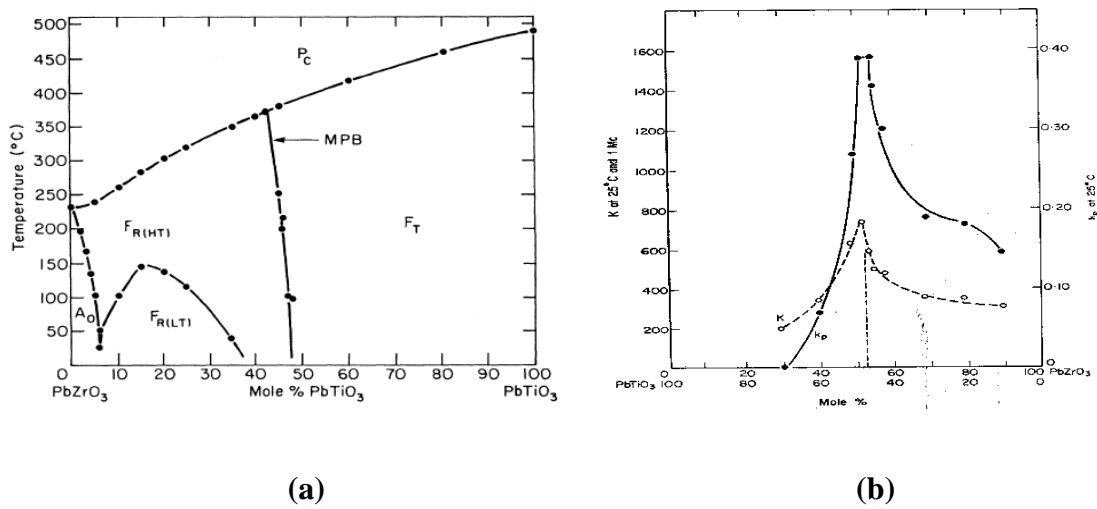
Fig.1.7 (a) Phase diagram of PZT piezoceramics (b) dielectric constant and planar coupling coefficient vs. composition [After Jaffe et al. (1971)].

But in past decade, presence of a monoclinic phase in the MPB region has been discovered in PZT and other MPB based solid solutions of the perovskite structure at room temperature [Fu et al. (2000); Noheda et al. (2000); Singh et al. (2003); Pandey et al. (2014)]. The phase diagram showing the presence of monoclinic phase around MPB for the PZT and PMN-PT piezoceramics is shown 1.8 (a) and Fig. 1.8 (b). Many other systems also show the presence of monoclinic phase around the morphotropic phase. It has been verified

experimentally [Guo et al. (2000); Noheda et al. (2002)] and theoretically [Fu et al. (2000); Vanderbilt et al. (2001)] that the monoclinic phase is present near the MPB composition of the peroskite structure. In the present Ph.D. work, Upadhyay and Singh (2015) also discovered a monoclinic (space group Pm) phase near the MPB composition of BMT-PT piezoceramics. Detailed results will be discussed in the chapter 3 of the thesis.
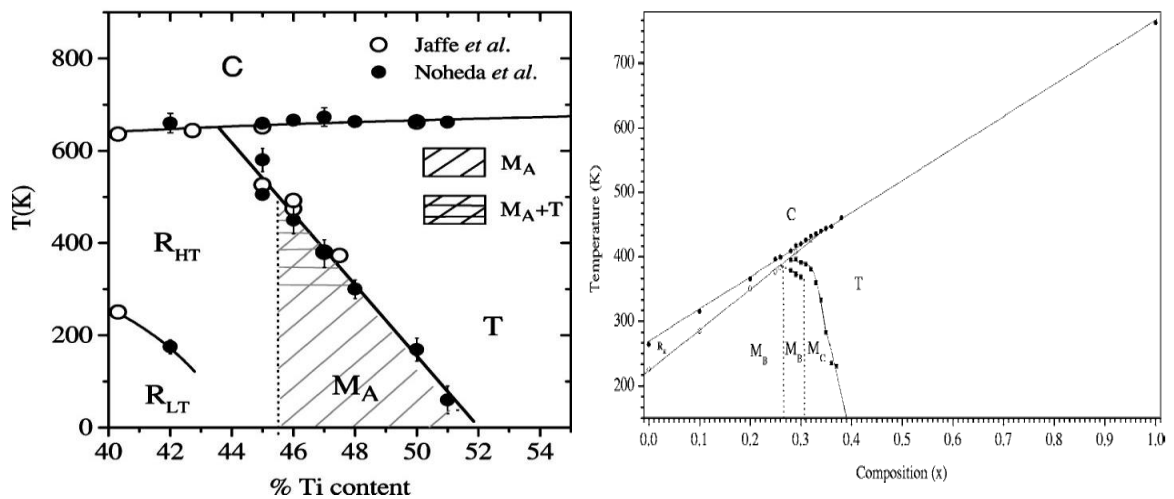
Fig.1.8 (a) Phase diagram of PZT [After Noheda et al. (2005)] and (b) PMN-PT [After Singh et al. (2006)].

1.10 Structure and properties of lead titanate system

Tetragonal perovskite lead titanate PbTiO$_3$ [PT] possesses large saturation polarization (Ps~81µC/cm^2) at room temperature [Jona et al. 1962] which is desirable for transducers applications. Synthesis of PT in dense ceramic form is not possible due to cubic to tetragonal phase transition and its large tetragonality (c/a=1.064) [Jaffe et al. (1971); Subbarao (1960)] as the materials disintegrate

18

while cooling below T_C (490ºC) after sintering. To reduce its tetragonality many efforts have been done either by chemical substitution on Pb^{2+} and Ti^{4+} site of PT or by adding some other perovskite of type $Pb(B_1 B_2)O_3$ or $Bi(B_1 B_2)O_3$. Many MPB based solid solutions were developed in the effort of decreasing tetragonality of PT.
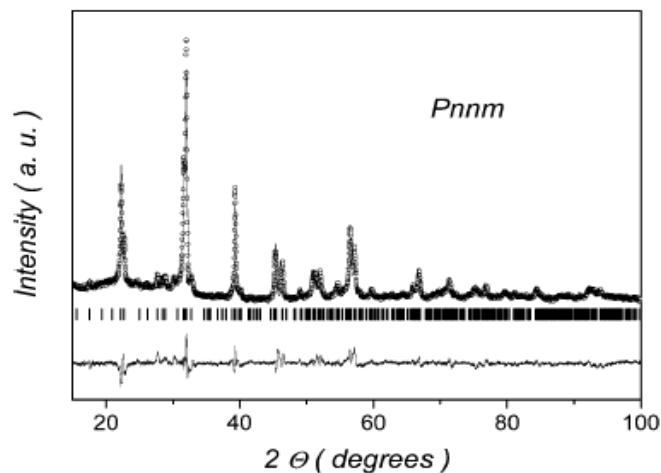
1.11 The BMT-PT solid solution system

The $(1-x)Bi(Mg_{1/2}Ti_{1/2})O_3-xPbTiO_3$ [BMT-PT] solid solution is a high temperature piezoelectric materials, which is suitable for many applications like actuators and transducers for space technology and automotive industries etc. Due to large tetragonality PT ceramic cannot be sintered, while for BMT high temperature and high pressure is required to prepare pure perovskite phase in ceramic form [Khalyavin et al. (2006); Yoneda et al. (2011)]. But together these two can be synthesised easily. BMT-PT appears to be most promising materials for high temperature piezoelectric applications with very high T_C~430°C, sufficient value of d_{33}~225pC/N, large tetragonality (c/a ~1.034) and large coercive field E_C~50kV/cm.

1.11.1 Preparation of BMT-PT solid solution

High temperature (1270K) and high pressure (6GPa) are required to synthesized phase pure perovskite structure of $(1-x)Bi(Mg_{1/2}Ti_{1/2})O_3$, the main component of BMT-PT piezoceramics, by conventional solid state ceramic route [Khalyavin et al. (2006); Yoneda et al. (2011)]. The BMT perovskite is a metastable phase which shows the orthorhombic structure (space group Pnnm) at high pressure. Rietveld fitted XRD pattern of BMT using Pnnm space group as

reported by Khalyavin is shown in Fig. 1.9 [Khalyavin et al. (2006); Yoneda et al. (2011)]. The main impurity phases detected by XRD after sintering of BMT were $Bi_{12}TiO_{20}$, $Bi_4Ti_3O_{12}$, and Mg_2TiO_4 [Khalyavin et al. (2006)]. There is an analogy between the crystal structure of BMT and anti-ferroelectric $PbZrO_3$ with respect to antiparallel shifts of A-site cation and oxygen octahedral tilting [Khalyavin et al. (2006); Suewattana et al. (2012)]. However BMT can be synthesized in single perovskite phase at ambient pressure by formation of its solid solutions with other ferroelectric perovskite with large tetragonality such as $PbTiO_3$ [Randall et al. (2004)], $Bi(Zn,Ti)O_3$ [Pushkarev et al. (2011)], $La(Mg,Ti)O_3$ [Salak et al. (2008)], and $BaTiO_3$ [Sun et al. (2010)].

In the present Ph.D. work the $(1-x)Bi(Mg_{1/2}Ti_{1/2})O_3-xPbTiO_3$ [BMT-PT] solid solution has been synthesised at ambient pressure and temperature in the composition range $0.28 \leq x \leq 0.45$ [Upadhyay et al. (2014)]. Detailed synthesis method for BMT-PT will be discussed in the chapter 3 of the thesis.

Fig.1.9 Observed (circles), calculated (continuous curve), and difference (solid line below the spectrum) room temperature powder XRD pattern of BMT synthesised at high pressure. The vertical bars correspond to the peak positions [After Khalyavin at al. (2006)].

1.11.2 Phase diagram of BMT-PT solid solution

$(1-x)Bi(Mg_{1/2}Ti_{1/2})O_3$-$xPbTiO_3$ [BMT-PT] polycrystalline ceramics have been investigated for the potential application in high temperature piezoelectric materials for the composition range $0.28 \leq x \leq 0.45$. Based on studies of BMT-PT ceramic sample several workers have reported the structure and phase diagram of the BMT-PT ceramics. The phase diagram reported by Randall et al. (2004) is shown in Fig. 1.10. As can be seen from the Fig. 1.10, high temperature paraelectric phase is cubic for all the compositions. The cubic to tetragonal phase transition temperature of the pure PT is lowered ($T_C \sim 430^{\circ}C$) with increasing content of BMT content. The cubic paraelectric phase is reported to transform into a rhombohedral phase at the BMT rich end.
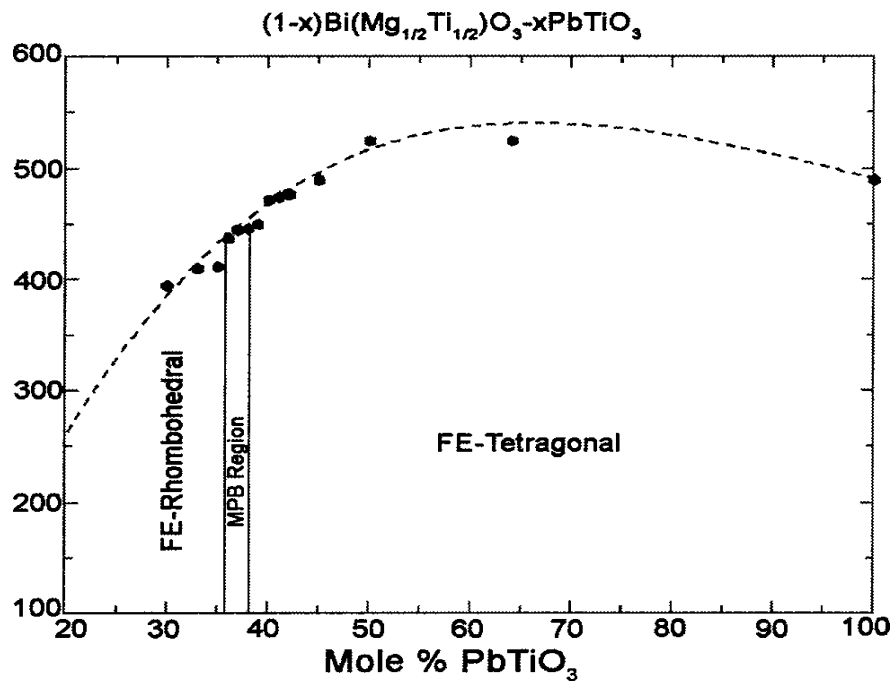
Fig.1.10 Temperatures vs. compositions phase diagram of BMT-PT system [After Randall et al. (2004)].

The rhombohedral and tetragonal phase field are separated by a morphotropic phase boundary (MPB) around the composition x~0.37. It was reported that the two phases coexists in MPB region. The piezoelectric response is found to be maximum near the morphotropic phase boundary composition with x~0.37 for the BMT-PT ceramics as shown in Fig 1.11(a) and Fig.1.11 (b) which shows the electromechanical coupling (k_{33}) coefficient and piezoelectric charge coefficient (d_{33}) [Randall et al. (2004); Chen et al. (2009)]. We will show in chapter 3 of this thesis that there is a monoclinic phase in MPB region of BMT-PT.
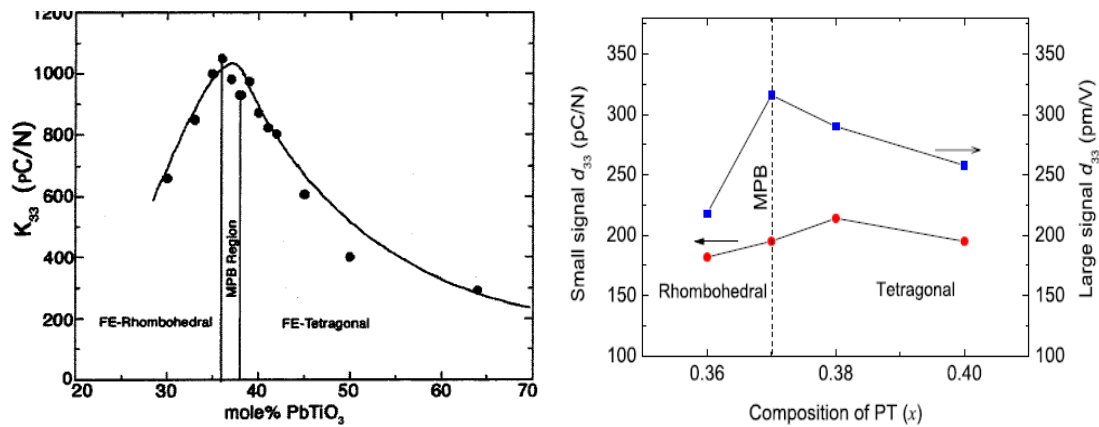
Fig.1.11 (a) Room temperature variation of k_{33} as a function of composition for BMT-PT [After Randall et al. (2004)], (b) composition dependence of piezoelectric coefficient d_{33} for BMT-PT [After Chen et al. (2009)].

1.11.3 Structure and phase coexistence in BMT-PT system

The structural characterisation of the MPB in (1-x)Bi(Mg$_{1/2}$Ti$_{1/2}$)O$_3$-xPbTiO$_3$ [BMT-PT] solid solution system have been investigated by several workers [Randall et al. (2004); Chen et al. (2009)]. It has been reported that the structure is predominantly rhombohedral for x≤0.36 whereas it is tetragonal for x≥0.38 at

room temperature. The morphotropic phase boundary is reported to lie around the composition with x~0.37. The coexistence of rhombohedral and tetragonal structures is reported for the MPB composition of BMT-PT [Randall et al. (2004)].

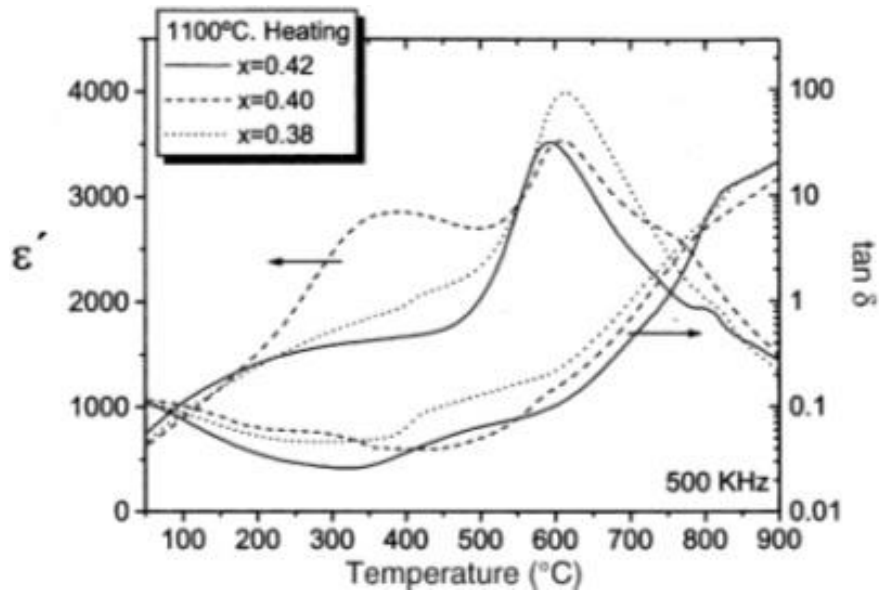## 1.11.4 Temperature dependent dielectric studies on BMT-PT

The temperature dependent dielectric studies on $(1-x)Bi(Mg_{1/2}Ti_{1/2})O_3$-$xPbTiO_3$ solid solution for several composition is reported by Suchomel and Davies is shown in Fig. 1.12 [Suchomel and Davies (2004)]. As can be seen from Fig 1.12, the Curie temperature increases with increasing the PT content. It has been shown that the MPB composition does not show the largest dielectric constant. The observed value of T_C~425°C found for MPB composition which is significantly higher than the value of T_C~385°C in PZT for the MPB compositions.
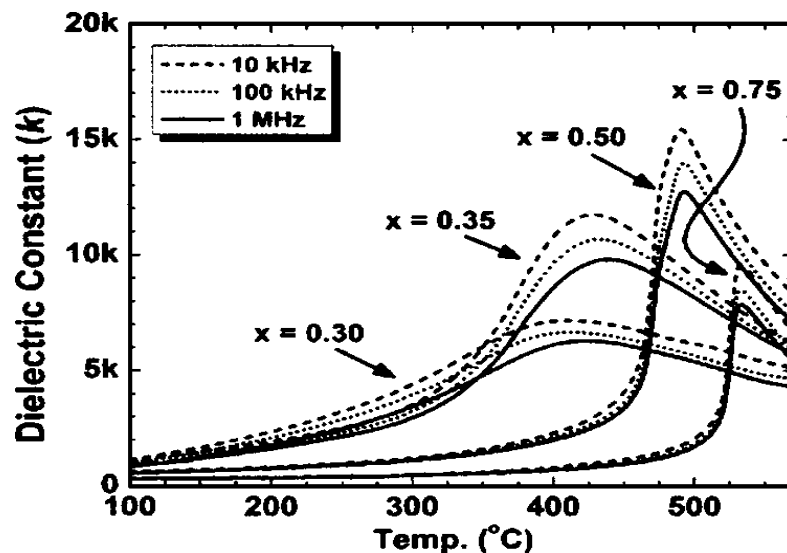
Fig.1.12 Dielectric constant measured at several frequencies plotted as a function of temperature for various compositions in the BMT-PT system [After Suchomel and Davies (2004)].

Fig.1.13 Dielectric permittivity and losses at 500 kHz as a function of temperature for BMT-PT ceramics sintered at 1100°C [After Moure et al. (2007)].

The temperature dependence of the dielectric permittivity and losses for the MPB composition of BMT-PT ceramics sintered at 1100°C reported by Moure et al. (2007) is shown in Fig 1.13. The well-defined maxima is observed with temperature for BMT-PT ceramics with composition x=0.38, 0.40, and 0.42. The dielectric anomaly is present for all the composition of BMT-PT. The anomaly at lower temperature at ~350°C probably associated with a second phase transition, which is ferroelectric to ferroelectric phase transition. There is another possibility of ferroelectric to anti-ferroelectric phase transition at ~350°C.

1.12 The BMZ-PT solid solution system

The $(1-x)Bi(Mg_{1/2}Zr_{1/2})O_3$-$xPbTiO_3$ [BMZ-PT] solid solution is also a high temperature piezoelectric material, which can be useful for actuators and transducers for space technology and automotive industries etc. [Qureshi et al. (2007)]. In this case also the preparation of $Bi(Mg_{1/2}Zr_{1/2})O_3$ in pure perovskite form of ceramics is not possible at ambient pressure and temperation. For the synthesis of BMZ in ceramic form, high temperature and high pressure is required. In case of BMZ-PT the paraelectric to ferroelectric phase transition occurred at value of (T_C)~280°C. The room temperature reported value of the remanent polarization (Pr) and coercive field (EC) were ~$29\mu C/cm^2$ and ~23kV/cm, respectively [Qureshi et al. (2007)]. BMZ-PT shows the high dielectric constant value ~1387 at room temperature near the morphotropic phase boundary region [Qureshi et al. (2007)].

1.12.1 Preparation of BMZ-PT solid solution

As discussed above, synthesis of phase pure BMT at ambient conditions is not possible. Similarly the preparation of BMZ is also not a possible in pure perovskite form. Formation of solid solutions with other stable perovskites such as $BaTiO_3$, $PbTiO_3$, etc. may be other approach to form the phase pure solid solution of BMZ at ambient pressure. We have synthesised the BMZ in phase pure perovskite form at ambient pressure by formation of its solid solutions with stable perovskites PT. The detailed preparation method has been discussed in chapter 5 of this thesis.

1.12.2 Structure, phase coexistence and phase diagram of BMZ-PT system

Recently the structure and dielectric properties of BMZ-PT solid solution have been studied [Shabbir et al. (2007); Qureshi et al. (2007)]. Shabbir et al. (2007) have reported that the MPB is found around the composition with x=0.54 to x=0.57, while Qureshi et al. (2007) have reported that the MPB is observed for the composition with x=0.55 to x=0.60. They have reported that the structure is predominantly rhombohedral for x≤0.55 whereas it is tetragonal for x≥0.65 at room temperature. The structure of the MPB composition was reported to be coexistence of rhombohedral and tetragonal phases [Shabbir et al. (2007); Qureshi et al. (2007)]. Suchomel and Davies (2004) have reported that the solid solution of BMZ-PT shows the cubic structure for the composition with x≤0.55 and tetragonal structure for the composition with structure x≥0.60. The morphotropic phase boundary region is observed for the intermediate composition of BMZ-PT piezoceramics [Suchomel et al. (2004)]. The Lattice parameters of BMZ-PT with composition and location of the phase coexistence region in the MPB composition reported by Suchomel et al (2004) is shown in Fig. 1.14. As can be seen from Fig. 1.14 the tetragonality increases with increasing the PT content. The structure of the BMZ-PT solid solution in the MPB region have not been investigated by Rietveld refinement for the confirmation of the structure. The composition vs. temperature phase diagram of BMZ-PT reported by Qureshi et al. (2007) is shown in Fig. 1.15. As can be seen from the Fig. 1.15, high temperature paraelectric phase is cubic for all the

compositions in phase diagram of BMZ-PT ceramics. The paraelectric cubic to ferroelectric tetragonal phase transition temperature of the pure PT is lowered ($T_C \sim 400^{\circ}C$) with increasing content of BMZ content. The cubic paraelectric phase is reported to transform into a ferroelectric rhombohedral phase at the BMZ rich end with Curie temperature $\sim 280^{\circ}C$. The ferroelectric rhombohedral and tetragonal phase field are separated by a morphotropic phase boundary (MPB) around the composition x~0.55. The piezoelectric response is found to be maximum near the morphotropic phase boundary composition with x~0.55 for the BMZ-PT ceramics. There is ambiguity in the structure and phase coexistence of the BMZ-PT piezoceramics as no detailed structural analysis of BMZ-PT piezoceramics have not been done so far.
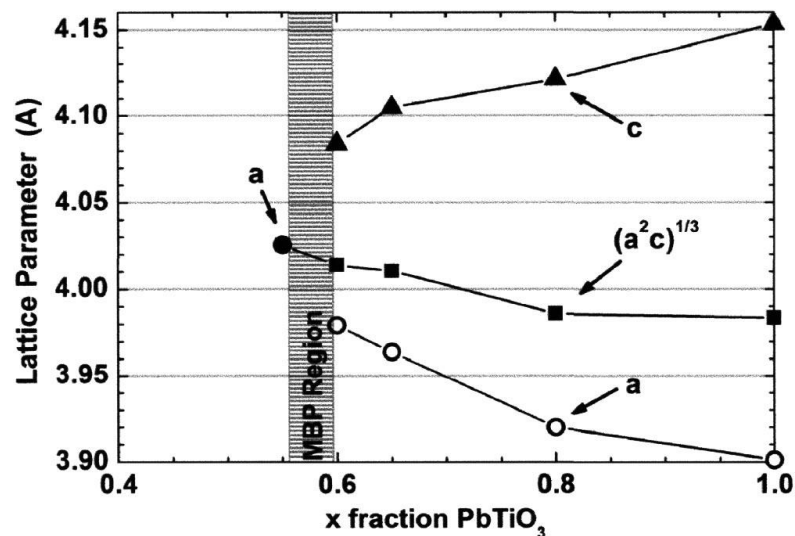

Fig.1.14 Variation of lattice parameters vs composition for $Bi(Mg_{1/2}Zr_{1/2})O_3$-$PbTiO_3$ system. Shaded area indicates the MPB region [After Suchomel et al. (2004)].
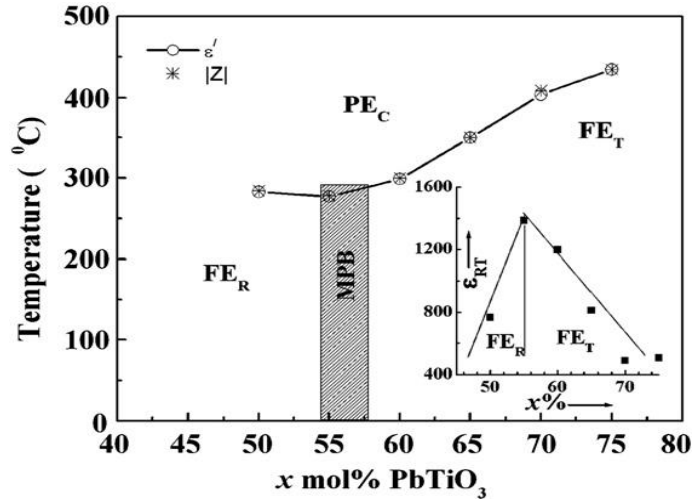
Fig.1.15 Phase diagram of the BMZ-PT ceramics constructed from the impedance (stars) and dielectric (open circles) data. Inset shows room temperature value of the dielectric constant vs $PbTiO_3$ concentration [After Qureshi et al. (2007)].

Polarization (P) - Electric field (E) hysteresis loop for the BMZ-0.55PT ceramics measured at room temperature is shown in Fig. 1.16. As can be seen from Fig. 1.16 a well saturated hysteresis loop is observed for the cubic composition of BMZ-PT ceramics also. It is somewhat unusual to get well saturated hysteresis loop in pseudocubic composition (x=0.55) of BMZ-PT. We will show in chapter 4, that such behaviour is observed due to an electric field induced phase transition. It is interesting to note that, the remnant polarization (Pr), for the cubic composition ($\sim 29\mu C/cm^2$) is comparable to that for tetragonal composition of BS-PT [Zhang et al. (2004); Shabbir et al. (2007)]. The large coercive field ($E_C \sim 23kV/cm$) is reported for the BMZ-PT piezoceramics. The large values of induced polarization and coercive filed (E_C) indicates strong ferroelectricity and stability of the BMZ-PT ceramic around the MPB composition.
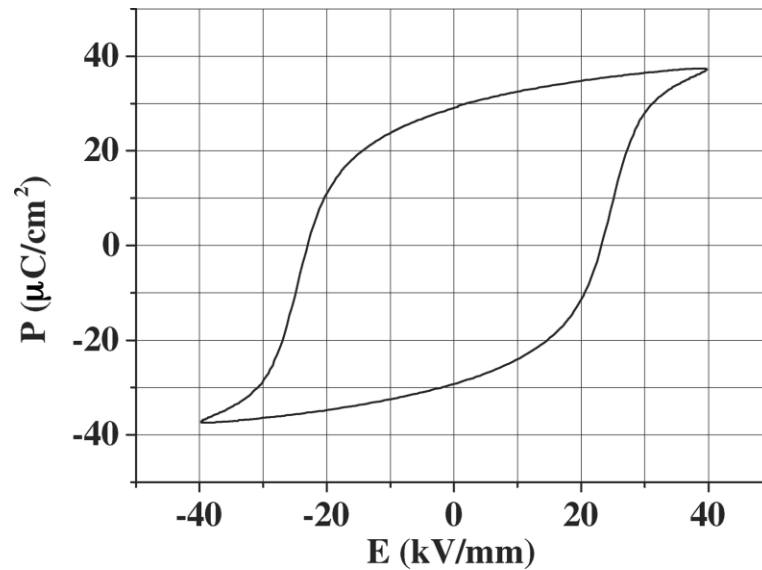
Fig.1.16 P-E hysteresis curve for the 0.45BMZ-0.55PT ceramics measured at room temperature [After Shabbir et al. (2007)].

1.12.3 Temperature dependent dielectric studies on BMZ-PT

The room temperature frequency dependent real (ε') and imaginary (ε'') parts of the complex dielectric permitivity of BMZ-PT ceramics for x = 0.57 and x = 0.56 reported by Shabbier et al. (2007) is shown in Fig. 1.17. The dielectric permittivity shows strong dispersion in the low frequency range for the both the composition of BMZ-PT ceramics. The significant value of the dielectric constant is observed for the BMZ-PT piezoceramics. Fig. 1.18 shows the temperature dependent dielectric constant of $(1-x)Bi(Mg_{1/2}Zr_{1/2})O_3-xPbTiO_3$ solid solution for several composition at different frequencies [Suchomel et al. (2004)].
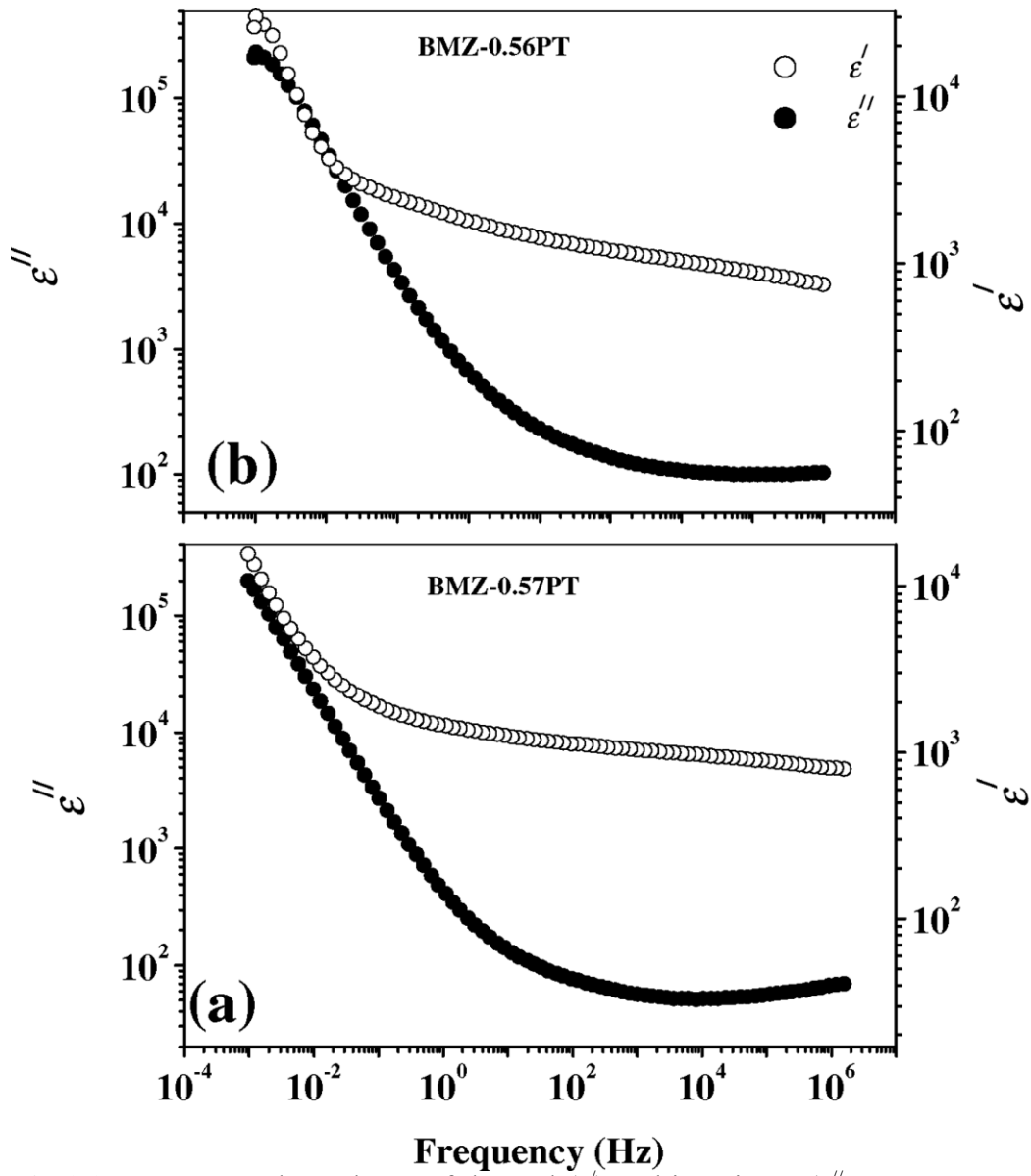
Fig.1.17 Frequency dependence of the real ($\varepsilon^{/}$) and imaginary ($\varepsilon^{//}$) parts of the complex dielectric constant of BMZ-PT ceramics at room temperature for (a) x=0.57 and (b) x=0.56 [After Shabbir et al. (2007)].

As can be seen from Fig 1.18, the Curie temperature increases with increasing the PbTiO$_3$ content like BMT-PT. It has been shown that the MPB composition does not show the largest dielectric constant. The observed value of T$_C$ found for MPB composition is lower than the value of T$_C$ of BMT-PT piezoceramics for the MPB composition [Suchomel et al. (2004)].
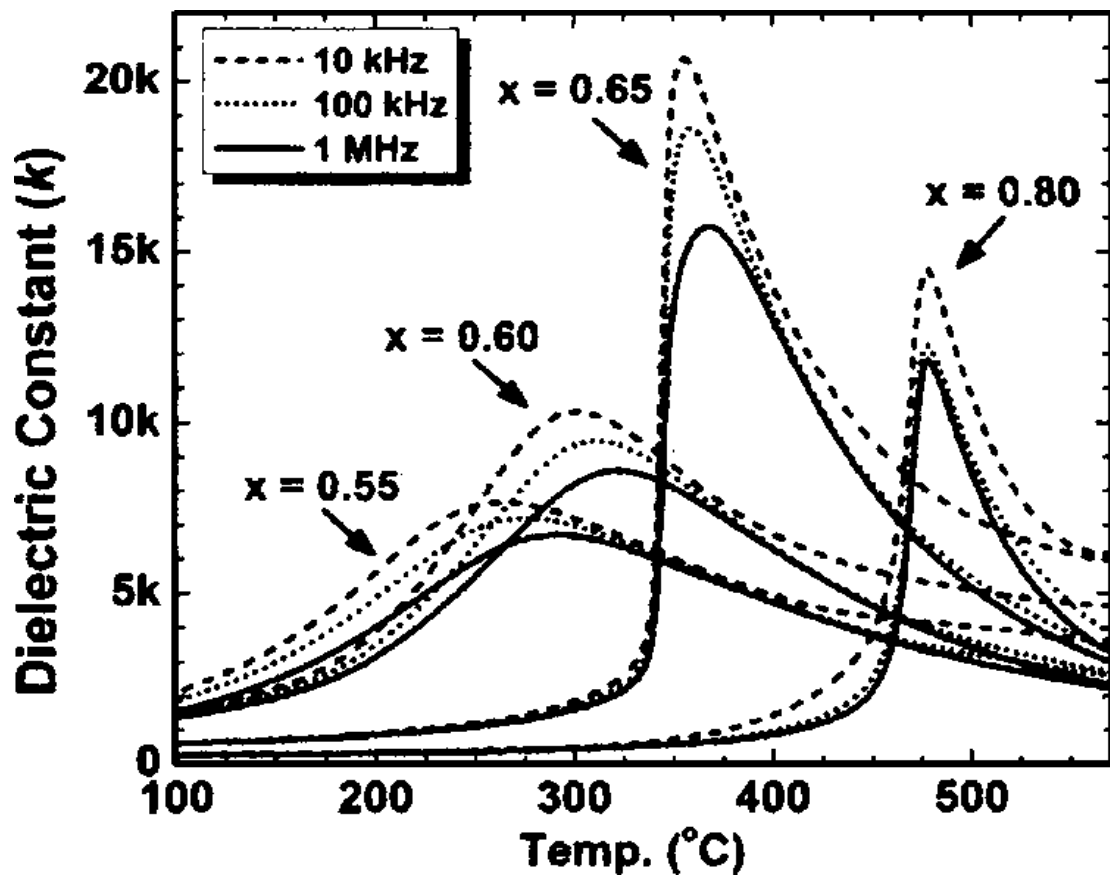

Fig.1.18 Dielectric constant measured at several frequencies as a function of temperature for various compositions of the (1-x)Bi(Mg$_{1/2}$Zr$_{1/2}$)O$_3$-xPbTiO$_3$ system [After Suchomel et al. (2004)].

1.13 Objective of the present work

Based on the detailed review of literature on new Bi-based MPB ceramics, the important objectives of the present Ph.D. work are as follow:

1. To synthesize phase pure perovskite solid solution of $Bi(Mg_{1/2}Ti_{1/2})O_3$ and $Bi(Mg_{1/2}Zr_{1/2})O_3$ with $PbTiO_3$.

2. To analyse the room temperature crystal structure of $(1-x)Bi(Mg_{1/2}Ti_{1/2})O_3$-$xPbTiO_3$ piezoceramics across MPB for the composition range $0.28 \leq x \leq 0.45$.

3. To locate the MPB region of $(1-x)Bi(Mg_{1/2}Ti_{1/2})O_3$- $xPbTiO_3$ piezoceramics.

4. To investigate the effect of grain size on the phase stability of $(1-x)Bi(Mg_{1/2}Ti_{1/2})O_3$- $xPbTiO_3$ piezoceramics.

5. To investigate the electric field induced phase transitions in $(1-x)Bi(Mg_{1/2}Ti_{1/2})O_3$- $xPbTiO_3$ piezoceramics.

6. To analyse the room temperature crystal structure of $(1-x)Bi(Mg_{1/2}Zr_{1/2})O_3$-$xPbTiO_3$ piezoceramics across MPB for the composition range $0.50 \leq x \leq 0.60$.

7. To investigate electric field induced phase transition in $(1-x)Bi(Mg_{1/2}Zr_{1/2})O_3$-$xPbTiO_3$ piezoceramics.

8. To understand the nature of phase transition below room temperature in $(1-x)Bi(Mg_{1/2}Ti_{1/2})O_3$-$xPbTiO_3$ and $(1-x)Bi(Mg_{1/2}Zr_{1/2})O_3$- $xPbTiO_3$ piezoceramics.

9. To investigate the phase stability in BMT-PT and BMZ-PT piezoceramics below room temperature.